# Initialization of iterative parametric algorithms for blind deconvolution of motion-blurred images

Vadim Loyev and Yitzhak Yitzhaky

Performances of iterative blind deconvolution methods for motion-blurred images are usually reduced depending on the accuracy of the required initial guess of the blur. We examine this dependency, and a two-stage restoration procedure is proposed: First we perform a direct technique with a single straightforward process to produce a rough initial estimate of the blur, and then an iterative technique is employed to refine the blur estimate. Two common iterative techniques (the expectation-maximization and the Richardson–Lucy methods) are examined here and implemented in the combined direct–iterative modification for a variety of motion blur types. Results show that the combined method significantly improves the reliability of the deconvolution process. 

*OCIS codes:* 100.1830, 100.3020.

## 1. Introduction

Blind image deconvolution (also called blind image restoration) refers to the problem of restoring images degraded by linear, space-invariant blur when the point-spread function (PSF) is unknown. Most of the recently developed blind deconvolution techniques are parametric and use an iterative procedure to estimate the blur and the ideal image. Motion blur, which results from a relative motion between the camera and the scene during exposure, is a common effect that degrades the image quality. Image stabilizing equipment usually has a limited capability and cannot completely prevent the effects of the motion.

Because the motion PSF that is necessary for the image restoration process is usually not known, a variety of blind deconvolution methods have been proposed in the past few decades. The limited success of these methods in real-life motion blur results mainly from the inaccuracies of the assumptions about the properties of the blur. These blind deconvolution methods can be classified into two types: direct and iterative. Direct methods[1–6] operate in a one-step fashion, which first estimates the blurring PSF and then uses the estimated PSF to restore the image with a restoration filter (such as the Wiener filter). Iterative methods[7–14] assume known models of the ideal image and the PSF, and in each step the image and the blur parameters are estimated and used in the next step. Both direct and iterative methods assume a linear space-invariant blurring process (a convolution model).

The earlier methods for blind blur estimation were direct[2–4] and assumed a uniform velocity motion in which a regular pattern of zero crossings is contained in the Fourier magnitude of its PSF. Since these zeros usually also appear in the power spectrum of the blurred image, spectral[2] and more robust cepstral[3,4] techniques were used to identify the PSF from the distance between the zeros in the power spectrum (or cepstrum) of the blurred image. Shortcomings of this approach are that the PSFs that do not satisfy these conditions cannot be identified and that the presence of noise in the observed image is not taken into account. A more recent direct method implemented in this work estimates the PSF's extent and direction[5] and also its shape.[6] This method will be described in Section 2.

Iterative methods usually formulate statistical models for both the image and the blur. During the restoration process the parameters of the models are estimated in an iterative process initiated with some guess of the desired parameters. The process ends when the estimated parameters maximize the appropriate likelihood function. Utilizing *a priori* knowledge about the blur may improve and accelerate the blind image restoration process in both iterative and direct methods. Furthermore, some blur types can be

The authors are with the Department of Electro-Optics Engineering, Ben Gurion University, Beer Sheva 84105, POB 653, Israel. Y. Yitzhaky's e-mail address is itzik@ee.bgu.ac.il.

Received 12 September 2005; revised 31 October 2005; accepted 6 November 2005; posted 7 November 2005 (Doc. ID 64756).

0003-6935/06/112444-09$15.00/0

defined by a few parameters only. In such cases blur identification is accomplished by identifying these parameters.[2–5,8] Examples of such sources of blur are uniform-velocity camera motion and being out of focus. Unfortunately, reliable knowledge about the motion blur is usually not available. The iterative algorithms require an initial guess of the PSF. As pointed out previously,[9] and as shown in this paper, the resulting accuracy of the estimated PSF (and consequently the quality of the restored image) depends on this guess. A closer guess usually leads to a more accurate estimation. Otherwise, the iterative algorithm may converge to a wrong extent estimation.[7,10] Some iterative algorithms also require an initial guess about the image model parameters, but it was shown[8] that the image model parameters are not essentially different from one image to the other and therefore may be guessed safely.

This paper examines the sensitivity of the iterative process to the accuracy of the PSF's initial guess and proposes an improvement of the reliability and accuracy of the blind deconvolution methods (both direct and iterative) by a combined direct–iterative process by first producing a more reliable initial PSF with a direct method, then used as the initial PSF guess by the iterative method. The direct blind deconvolution method used[5,6] was shown to be relatively most robust in the task of PSF estimation among other direct methods.[1] The iterative blind deconvolution methods that are examined and employed here are commonly known as the expectation-maximization (EM)[9] and the Richardson–Lucy (RL)[11–13] methods.

The rest of the paper is organized as follows: Section 2 briefly presents the image restoration methods used here, where the direct method used for the initial blur estimation is described in Subsection 2.A and the iterative methods used to refine the blur estimation and to restore the image are described in Subsection 2.B. The sensitivity of the iterative methods to the accuracy of the initial guess is examined in Section 3. The combined direct–iterative method proposed here is presented in Section 4, and comparative blur estimation results and image restoration results are presented in Section 5. Conclusions are given in Section 6.

## 2. Direct and Iterative Image Restoration Methods

### A. Direct Methods

In direct blind deconvolution methods the PSF estimation and the deconvolution process are done consecutively and straightforwardly in one step. No mathematical criterion is used to evaluate the estimation. However, the absence of such a criterion does not necessarily indicate a less successful estimation. In the case of motion blur, most of the restoration techniques assumed a uniform-velocity motion during the exposure. In such a motion type, the blur identification process is relatively simple, since the blur can be determined only by its extent and direction, and these parameters are relatively easier to be identified from the blurred image. The problem with such an assumption is that in many practical situations it is not true. The direct method used here[5,6] does not assume such a knowledge of the motion type.

Summarizing this method, operations of high-pass filtering and averaging are used to significantly decrease the correlation properties of the original image so that the remaining information characterizes primarily the correlation properties of the PSF. Both PSF parameters (extent and direction)[5] and a PSF shape[6] are estimated by this method. The PSF extent is the size of the motion-induced smear at the image plane (usually in pixel units). This extent is defined as the distance between the steepest ascent and the steepest descent of the PSF. Its direction is the angle of that smear relative to the horizontal image axis. The PSF shape is the distribution of the response to a point object (with an intensity equal to one), which is proportional to the inverse of the instantaneous motion velocity at each location along the smear. A common motion blur property of one dimensionality of the PSF is assumed and exploited. The first necessary step of the method is identification of the motion direction. The motion during exposure affects the image by decreasing its resolution mostly in the motion direction. Assuming an approximately isotropic spectrum of the average subsections of the unblurred image, the direction is identified by an average of partially overlapped subsections of the blurred image and extraction of the direction whereby the image resolution is maximally decreased. This can be done by high-pass filtering of the blurred image in all directions (in steps of 1 deg, for instance) and measuring of the intensity of the filtered image in each case. The blur direction is the one where the intensity is the lowest. A high-pass filter can be obtained by means of a simple derivative operation. The next step is an implementation of a high-pass filter in the motion direction and perpendicular to it. Implementation of such a filter will form patterns similar to the high-pass-filtered PSF, surrounded by extremely suppressed decorrelated (pseudowhitened) regions. The filtered image in the Fourier domain $\Delta G(u, v)$ can be formulated as

$$\Delta G(u, v) = G(u, v)W(v)W(u), \tag{1}$$

where $W(v)$ and $W(u)$ are the high-pass filters perpendicular to and in the motion direction (that coincide with the $u$ axis). These PSF-like patterns are evaluated by first implementing an autocorrelation operation to all the filtered image lines $l(j)$ in the motion direction,

$$R_l(j) = \frac{1}{M}\sum_{i=-M}^{M} l(i+j)l(i), \quad \text{integer}\, j \in [M, -M],$$

$$l(i) = 0 \quad \text{for}\, i \notin [0, M], \tag{2}$$

and then averaging them to suppress the noise stimulated by the high-pass-filtering operations. Furthermore, such averaging will cause cancellation of correlation properties remaining from the original image that can be different from one line to another.

For many motion blur cases, the blur extent is the distance between the center of the average autocorrelation function (ACF) and its global minimum.[5] Since the ACF is usually similar to the autocorrelation of the filtered PSF, the discrete Fourier transform (DFT) of the average autocorrelation, $\bar{S}_{\Delta G}$, is also similar to the power spectrum of the filtered PSF, i.e.,

$$\bar{S}_{\Delta G} \approx S_{\Delta \mathrm{PSF}}, \tag{3}$$

where

$$S_{\Delta \mathrm{PSF}} = |HW(u)|^2, \tag{4}$$

and $H$ is the Fourier transform of the PSF, which is actually the optical transfer function (OTF) of the motion-blurring system.[15] The modulation transfer function (MTF) of the blur is the absolute value of the OTF and can be approximated from Eqs. (3) and (4) by[6]

$$\mathrm{MTF}(u) \approx \frac{\left[\bar{S}_{\Delta G}(u)\right]^{1/2}}{|W(u)|}. \tag{5}$$

For causal blur processes the phase transfer function (PTF) and is related to the MTF by

$$\mathrm{PTF}(u) = \frac{1}{2\pi}\int_0^{2\pi} \ln[\mathrm{MTF}(\alpha)]\cot\frac{u-\alpha}{2}\,\mathrm{d}\alpha. \tag{6}$$

The OTF used to restore the blurred image is obtained by

$$H = \mathrm{MTF}\exp(j\mathrm{PTF}). \tag{7}$$

The estimated PSF is then obtained by an inverse Fourier transform of the identified OTF.

### B. Iterative Methods

As stated earlier, from a variety of iterative blind deconvolution methods,[7] we chose two major methods, the EM[9] and the RL[11–13] methods, for the examination of and incorporation in the proposed direct–iterative blind deconvolution process.

The observed image $g(i, j)$ is modeled as the output of a two-dimensional (2-D) finite impulse response linear space-invariant system[10]:

$$g(i, j) = \sum_{m,n\in S_h} h(m, n) f(i-m, j-n) + \omega(i, j), \tag{8}$$

where $i, j$ represent the vertical and horizontal coordinates, respectively; $f(i, j)$ is the ideal image, $h(m, n)$ is the blurring PSF; $S_h$ is the support of the PSF; and $\omega(i, j)$ is the observation noise, assumed to be an additive zero-mean homogeneous process with a Gaussian distribution and a covariance $Q_\omega(i, j) = \sigma_\omega^2\,\delta(i, j)$.

Since the motion-blurring process is assumed not to reduce or generate energy, the PSF should satisfy

$$\sum_{m,n\in S_h} h(m, n) = 1. \tag{9}$$

Furthermore, since both the original and the observed images represent intensity distributions that do not contain negative values, the PSF coefficients are nonnegative.

A more compact notation for Eq. (8) can be derived using a lexicographical representation of the original and the blurred images by stacking the image data into a vector through conventional raster scanning:

$$g = Hf + \omega, \tag{10}$$

where the vectors $g$, $f$, and $\omega$ are the $N^2 \times 1$ lexicographical representations of $g(i, j)$, $f(i, j)$, and $\omega(i, j)$, and $H$ is an $N^2 \times N^2$ matrix formed by the PSF coefficients.

#### 1. Richardson–Lucy Deconvolution

Starting with Eq. (8), and dropping the observation noise term, the RL[11–13] method continues with a Bayesian postulate:

$$P(f_i|g_k) = \frac{P(g_k|f_i)P(f_i)}{\sum_j P(g_k|f_j)P(f_i)};$$

$$i = \{1, I\},\ j = \{1, J\},\ k = \{1, K\}, \tag{11}$$

where $g_k$ and $f_i$ are arbitrary cells of $g$ and $f$, respectively. Developing the algorithm in a Bayesian way leads eventually to the following iterative image restoration procedure[8,11]:

$$\hat{f}_1(i, j) = \sum_{m=i}^{i+K-1}\sum_{n=j}^{j+L-1} \frac{g(m, n)\hat{h}_1(m-i+1, n-j+1)}{\sum_{p=a}^{b}\sum_{q=c}^{d}\hat{h}_1(m-p+1, n-q+1)}, \tag{12}$$

$$\hat{f}_{r+1}(i, j) = \hat{f}_r(i, j)\sum_{m=i}^{i+K-1}\sum_{n=j}^{j+L-1} \frac{g(m, n)\hat{h}_r(m-i+1, n-j+1)}{\sum_{p=a}^{b}\sum_{q=c}^{d}\hat{f}_r(p, q)\hat{h}_r(m-p+1, n-q+1)}, \tag{13}$$

where $(K, L)$ are the dimensions of $h$, $(I, J)$ are dimensions of $f$, $a = (1, m - K + 1)_{\max}$, $b = (m, I)_{\min}$, $c = (1, n - L + 1)_{\max}$, $d = (n, J)_{\min}$, $i = \{1, I\}$, $j = \{1, J\}$, $k = \{1, K\}$, and $l = \{1, L\}$.

Equation (13) can be formulated in a more compact form[13]:

$$\hat{f}_{r+1} = \hat{f}_r \left( \hat{h}_r * \frac{g}{\hat{h}_r \otimes \hat{f}_r} \right) \equiv \Psi(\hat{f}_r), \tag{14}$$

where $\hat{f}_r$ is the restored image after $r$ iterations, $*$ is the correlation operator, and $\otimes$ is the convolution operator.

The estimated PSF $\hat{h}_r$ is found in a similar way[13] (although its initial value $\hat{h}_1$ should be guessed):

$$\hat{h}_{r+1} = \hat{h}_r \left( \hat{f}_r * \frac{g}{\hat{h}_r \otimes \hat{f}_r} \right) \equiv \Omega(\hat{h}_r), \tag{15}$$

where $\hat{f}_{r+1}$ and $\hat{h}_{r+1}$ are estimated in each iteration separately. It is also possible to accelerate the algorithm by choosing[13]

$$\begin{aligned} \hat{f}_{r+\lambda} &= \hat{f}_r + \lambda_f \left[ \Psi(\hat{f}_r) - \hat{f}_r \right], \\ \hat{h}_{r+\lambda} &= \hat{h}_r + \lambda_h \left[ \Omega(\hat{h}_r) - \hat{h}_r \right], \end{aligned} \tag{16}$$

where

$$\lambda_f = \frac{\sum_i^N \sum_j^N \left\{ \left[ \hat{f}_{r+1}(i, j) - \hat{f}_r(i, j) \right] \left[ \hat{f}_r(i, j) - \hat{f}_{r-1}(i, j) \right] \right\}}{\sum_i^N \sum_j^N \left\{ \left[ \hat{f}_r(i, j) - \hat{f}_{r-1}(i, j) \right]^2 \right\}}, \tag{17}$$

$$\lambda_h = \frac{\sum_i^N \sum_j^N \left\{ \left[ \hat{h}_{r+1}(i, j) - \hat{h}_r(i, j) \right] \left[ \hat{h}_r(i, j) - \hat{h}_{r-1}(i, j) \right] \right\}}{\sum_i^N \sum_j^N \left\{ \left[ \hat{h}_r(i, j) - \hat{h}_{r-1}(i, j) \right]^2 \right\}}. \tag{18}$$

*2. Expectation-Maximization Deconvolution*

The original image in most methods[7–10] is modeled and expressed by a 2-D homogeneous Gauss–Markov process represented by the following 2-D autoregressive model:

$$f(i, j) = \sum_{k,l \in S_a} a(k, l) f(i - k, j - l) + \nu(i, j), \tag{19}$$

where $a(k, l)$ are the image model coefficients, and $S_a$ is the causal (quarter-plane)[9] or the nonsymmetric half-plane[8] model support. The modeling error $\nu(i, j)$ is a zero-mean homogeneous Gaussian-distributed white-noise process with covariance $Q_\nu(i, j) = \sigma_\nu \delta(i, j)$ and is independent of $f(i, j)$. It is assumed that the coefficients $a(k, l)$ are chosen in such a way that Eq. (19) is a stable image model.[10] Similarly to Eq. (10), the more compact notation of Eq. (19) is obtained using a lexicographic representation,

$$f = Af + \nu, \tag{20}$$

where $A$ is a matrix formed by the image model coefficients and the vector $\nu$ is a lexicographic representation of $\nu(i, j)$.

To derive a restoration filter to obtain an estimate of $\hat{f}$ that is as close as possible to the original image $f$, the PSF $h(m, n)$, the variance of the observation noise $\sigma_\omega^2$, and the model of the original image [$a(k, l)$ and $\sigma_\nu^2$] need to be accurately estimated.

It is common to denote the unknown parameters by a vector $\theta$:

$$\theta = (\theta_1, \theta_2, \ldots, \theta_M)^t = \left[ h(m, n), a(k, l), \sigma_\omega^2, \sigma_\nu^2 \right]. \tag{21}$$

The maximum-likelihood estimator of the parameter vector $\theta$ is defined by[9]

$$\hat{\theta}_{\mathrm{ml}} = \arg\left\{ \max_{\theta \in \Theta} L^*(\theta) \right\} = \arg\left\{ \max_{\theta \in \Theta} \log p(g; \theta) \right\}, \tag{22}$$

where $p(g; \theta)$ is the *a priori* probability density function (PDF) of the observed image, given the $\theta$; $L^*(\theta)$ is the (log)-likelihood function of $\theta$; and $\Theta$ specifies the range of the parameters $\theta$.

The PDF of $g$, $p(g; \theta)$ is derived through the PDF of $f$, $p(f; A, Q_\nu)$, given the model parameters and assuming zero-mean homogeneous Gaussian characteristics of $\nu$:

$$p(f; A, Q_\nu) = \left[ \frac{\det|I - A|^2}{2\pi^{N^2} \det|Q_\nu|} \right]^{1/2} \times \exp\left[ -\frac{1}{2} f^t (I - A)^t Q_\nu^{-1} (I - A) f \right]. \tag{23}$$

Given the PDF of $g$, $p(g/f; H, Q_\omega)$, the PDF of the observation noise, the model for the blurring system, and the original image,

$$p(g/f; H, Q_\omega) = \frac{1}{\sqrt{2\pi^{N^2} \det|Q_\omega|}} \times \exp\left[ -\frac{1}{2} (g - \mathrm{H}f)^t Q_\omega^{-1} (g - Hf) \right], \tag{24}$$

where $Q_\nu = \sigma_\nu^2 I$ is the covariance matrix of the modeling error $\nu$, and $Q_\omega = \sigma_\omega^2 I$ is the covariance matrix of the observation noise $\omega$.

By combining Eqs. (23) and (24), dropping all constant terms, and premultiplying the result by $-2$ [the maximization in Eq. (22) now becomes a minimization], we obtain the equivalent likelihood function

$L(\theta)$:

$$L(\theta) = \log(\det|P|) + g^t P^{-1} g, \tag{25}$$

where

$$P = \mathrm{cov}(g) = \sigma_v{}^2 H(I-A)^{-1}(I-A)^{-1}H^t + \sigma_\omega{}^2 I. \tag{26}$$

One of the considerations in modeling images is that images are always of finite extent. As a result, Eqs. (10) and (20) cannot model the data near the boundaries of the image accurately. We therefore have to preprocess the observed blurred image around its boundaries such that Eq. (10) is consistent with either circular or linear convolution of $h(i, j)$ and $f(i, j)$. Linear convolution in Eqs. (10) and (20) enforces the observation matrix $H$ and the image model matrix $A$ to be block Toeplitz. The circular convolution in Eqs. (10) and (20) leads to the block-circulant $H$ and $A$ matrices. If the matrices $H$ and $A$ are assumed to have a block-circulant structure, $P$ has a block-circulant structure as well. Associated with $P$ is the following 2-D convolution kernel $p(i, j)$:

$$p(i, j) = \sigma_v{}^2 h(i, j)[1 - a(i, j)]^{-1}[1 - a(-i, -j)]^{-1} \times h(-i, -j) + \sigma_\omega{}^2. \tag{27}$$

All the matrices in Eq. (27) commute because they are related to convolutions. The covariance matrix $P$ is positive definite provided that $\sigma_\omega{}^2 > 0$ (nonzero noise exists in the degraded image). As a consequence, the inverse of $P$ and the logarithm of $\det|P|$ always exist.

It should be noted that the dimensions of $P$ are $N^2 \times N^2$, where typical values of $N$ are 128, 256, or even larger. Hence direct evaluation of Eqs. (26) and (27) may not be feasible in practice.

However, if we assume that the matrices $A$ and $H$ are block circulant, then they can be diagonalized by employing a 2-D DFT.[16] The eigenvalues of $A$, $H$, and $P$ are given by the DFT coefficients corresponding to $a(k, l)$, $h(m, n)$, and $p(i, j)$, respectively.

Any likelihood function $L(\theta)$ can be optimized by the following iterative scheme[12]:

$$L(\theta; \hat{\theta}^{(k)}) = E\{\log p(X; \theta)/Y; \hat{\theta}^{(k)}\}, \tag{28}$$

$$\hat{\theta}^{(k+1)} = \arg\Big\{\max_{\theta\in\Theta} L(\theta; \hat{\theta}^{(k)})\Big\}, \tag{29}$$

where $L(\theta; \hat{\theta}^{(k)})$ is the conditional likelihood function. The above iterations are known as the EM algorithm, where Eqs. (28) and (29) are called the E-step and the M-step, respectively. In Eq. (28) $X$ denotes an appropriately chosen complete data set, which includes the observed incomplete data $Y$ as a subset. For the image blur identification problem, $X = \{f, g\}$ and $\hat{Y} = \{g\}$ were chosen.[9] Substituting the above choice of $X$ and $Y$ into the EM algorithm, together with the models described here, lead to the following iteration[9,10] for the E-step:

$$V^{(k)} = \mathrm{cov}(f/g; \theta^{(k)}) = \big[(I-A)^t Q_v{}^{-1}(I-A) + H^t Q_\omega{}^{-1} H\big]^{-1}, \tag{30}$$

$$\hat{f}^{(k)} = E(f/g; \theta^{(k)}) = V^{(k)} H^t Q_\omega{}^{-1} g; \tag{31}$$

and to the following for the M-step:

$$\hat{r}_{ff}{}^{(k)}(p, q) = \sum_{k,l\in S_a} \hat{a}(k, l)\hat{r}_{ff}{}^{(k)}(p-k, q-l), \quad \forall (p, q) \in S_a, \tag{32}$$

$$\hat{\sigma}_v{}^2 = \hat{r}_{ff}{}^{(k)}(0, 0) - \sum_{k,l\in S_a} \hat{a}(k, l)\hat{r}_{ff}{}^{(k)}(k, l), \tag{33}$$

$$\hat{r}_{fg}{}^{(k)}(-p, -q) = \sum_{m,n\in S_h} \hat{h}(m, n)\hat{r}_{ff}{}^{(k)}(p-m, q-n), \quad \forall (p, q) \in S_h, \tag{34}$$

$$\hat{\sigma}_\omega{}^2 = \frac{1}{N^2}\sum_{i,j=1}^{N} g(i, j)^2 - \sum_{m,n\in S_h} \hat{h}(m, n) \times \hat{r}_{fg}{}^{(k)}(-m, -n), \tag{35}$$

where $\hat{r}_{ff}{}^{(k)}(p, q)$ and $\hat{r}_{fg}{}^{(k)}(p, q)$ are the defining bisequences of the conditional autocorrelation matrix $\hat{R}_{ff}{}^{(k)}$ and cross-correlation matrix $\hat{R}_{fg}{}^{(k)}$, respectively,[9] and $V^{(k)}(p, q)$ below is the defining bisequence of $V^{(k)}$:

$$\hat{r}_{ff}{}^{(k)}(p, q) = V^{(k)}(p, q) + \frac{1}{N^2}\sum_{i,j=1}^{N} \hat{f}^{(k)}(i, j) \times \hat{f}^{(k)}(i-p, j-q), \tag{36}$$

$$\hat{r}_{fg}{}^{(k)}(p, q) = \sum_{i,j=1}^{N} \hat{f}^{(k)}(i, j) g^{(k)}(i-p, j-q). \tag{37}$$

### 3. Sensitivity of the Iterative Methods to the Accuracy of the Initial Guess

As postulated earlier, the estimation quality of the iterative procedures depends on the accuracy of the initial PSF guess.[7] This dependence was examined experimentally for various initial PSF types and different images. One typical example of this examination by use of the original cameraman image shown in Fig. 1 is presented in Table 1. Table 1 presents comparisons between true and estimated PSFs for various initial PSF guesses, using the EM and RL methods. Each column in Table 1 shows a true PSF, an initial PSF, and the PSFs estimated by the RL and the EM methods (obtained with 100 iterations). The rightmost column presents the average mean square error (MSE) between the true and the other PSFs. It can be seen from these examples that in both methods the accuracy of the estimated PSF depends on the accuracy of the ini-

Fig. 1. Original cameraman image used in the simulation examples (256 × 256 pixels).

tial PSF. In the top part of Table 1 this dependency is shown for the same blur extent but for different initial shape guesses. The true blurring PSF is a 3-pixel square function (which is a PSF of a uniform-velocity motion), whereas the initial PSFs have the same extent but with various distributions. The bottom part of Table 1 shows this dependency for the same PSF shapes (square functions) but for different initial PSF extents (4, 5, and 6 pixels). It was found that the iterative methods are more sensitive to errors in the PSF extent than to errors in its shape, since a higher average MSE is shown in the case of extent errors (bottom part of Table 1). This is important because in various cases the PSF extent is easier for estimation.[2–5,8] The direct method used here to produce the initial PSF gives an estimation of both its shape and extent.

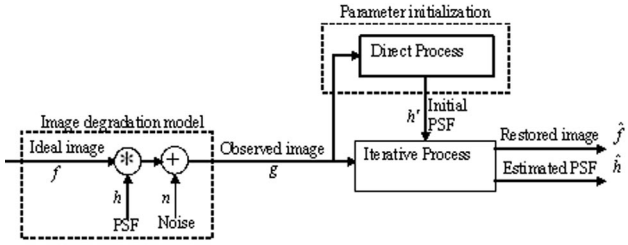


Fig. 2. Block diagram of the degradation and the combined direct–iterative blind deconvolution processes.

## 4. Combined Direct–Iterative Method

Figure 2 presents a block diagram of the degradation model [Eq. (8)] and the basic proposed direct–iterative blind deconvolution process. The degradation is modeled by a convolution of the ideal image $f$ with the motion blur PSF $h$ and an additive noise $n$. The blind deconvolution process begins with estimating the initial blurring PSF $h'$ by the direct method and continues with the iterative process initialized by this PSF, which produces the final (refined) estimated PSF $\hat{h}$ and the restored image $\hat{f}$. In Section 5 we present comparative implementation results of this proposed direct–iterative blind deconvolution process, where the iterative process is the EM method[9] or the RL method[10–13] and the direct process is the pseudo-whitening method.[5,6]

**Table 1. Sensitivity of the Iterative Process (with 100 Iterations) to the Initial Point-Spread Function Guess (Cameraman Image)[a]**

| Process | True, Initial, and Estimated PSFs | | | | | Average MSE |
|---|---|---|---|---|---|---|
| Sensitivity to unknown initial shape[b] | | | | | | |
| True PSF | 33, 33, 33 | 10, 80, 10 | 60, 30, 10 | 20, 40, 40 | 40, 20, 40 | |
| Initial guess | 33, 33, 33 | 10, 80, 10 | 60, 30, 10 | 20, 40, 40 | 40, 20, 40 | 0 |
| RL | 33, 33, 33 | 10, 80, 10 | 60, 30, 10 | 20, 40, 40 | 40, 20, 40 | 0 |
| EM | 33, 33, 33 | 13, 73, 13 | 60, 30, 10 | 20, 40, 40 | 40, 20, 40 | 0.5 |
| Initial guess | — | 33, 33, 33 | 33, 33, 33 | 33, 33, 33 | 33, 33, 33 | 10.5 |
| RL | — | 29, 43, 28 | 41, 38, 21 | 31, 38, 31 | 36, 28, 35 | 7.9 |
| EM | — | 18, 64, 18 | 22, 56, 22 | 31, 36, 33 | 40, 20, 40 | 6.7 |
| Sensitivity to unknown initial blur extent[c] | | | | | | |
| True PSF | 33, 33, 33 | 33, 33, 33 | | 33, 33, 33 | | |
| Initial guess | 25, 25, 25, 25 | 20, 20, 20, 20, 20 | | 16, 16, 16, 16, 16, 16 | | 11.7 |
| RL | 22, 30, 30, 18 | 17, 25, 28, 19, 11 | | 13, 19, 20, 19, 18, 11 | | 9.5 |
| EM | 23, 25, 30, 22 | 12, 23, 31, 19, 14 | | 12, 24, 22, 19, 10, 13 | | 8.8 |

[a]Values are multiplied by 100 for compact representation.
[b]Extent is known.
[c]Shape is known.

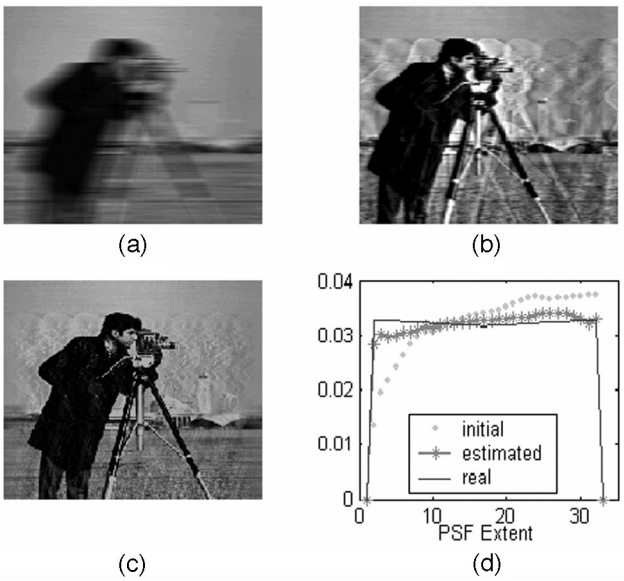


Fig. 3. (a) Cameraman image degraded by a 33-pixel portion of a low-frequency sinusoidal motion blur; (b) image restored by a direct method; (c) image restored by the proposed direct–iterative RL method; and (d) real, initial, and final estimated PSFs.

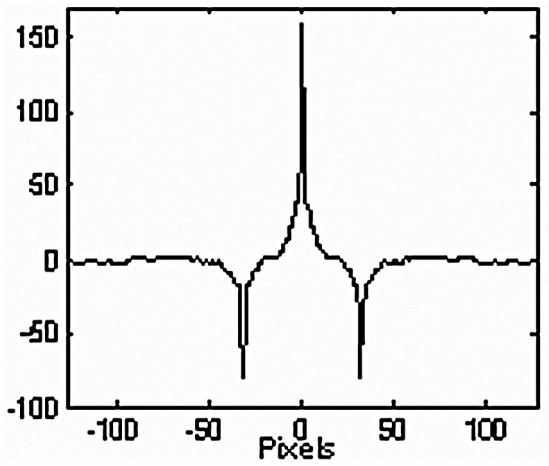


Fig. 4. Average ACF that produces the initial PSF estimation of the direct method from the blurred image of Fig. 3(a). The distance between a global minimum and the center of the ACF (33 pixels in this case) is the blur extent estimation of the direct method.

### 5. Point-Spread Function Estimation and Image Restoration Results

The proposed direct–iterative method was applied to both simulated and real-motion-blurred images. In the simulations where different motion types were employed, the estimated PSF can be compared with the known true PSF. In cases of real-degraded images, where the true PSF is unknown, the estimated PSF is evaluated according to the quality of the restored image (as the restoration is frequently the purpose of the estimation). Such an evaluation is usually done subjectively by viewing and comparing the restored and the degraded images. When no knowledge exists about the original image and about the image distortion properties, mathematical image quality measures are rarely used and have limited success because of the lack of knowledge about the desired properties of the restored image.[17–19] The cameraman image shown in Fig. 1 was used as the original image in the simulation examples presented in Figs. 3–6. Motion blur types were chosen to be different cases of the common sinusoidal motion blur because of the large variety of PSFs associated with this motion type.[20] The PSF of a sinusoidal motion blur depends on parameters such as the proportion between the exposure and the sine-wave period and the phase of the sine wave in which the exposure has started. A case in which the exposure is smaller than the sinusoidal period is called low-frequency vibrations.[15]

In Fig. 3(a) the original image was blurred by a portion of the sinusoidal motion with a PSF that is similar to that of a uniform-velocity motion. The average ACF [Eq. (2)] that produces the initial PSF estimation [Eqs. (3)–(7)] is shown in Fig. 4. The distance between a global minimum and the center of the ACF is the blur extent estimation of the direct method, which is used as the extent of the initial PSF (the blur extent). Figure 3(b) shows the image restored by the direct method using the initial estimated PSF (as described in Subsection 2.A). Figure 3(c) shows the image restored by the RL method, given the directly estimated initial PSF and 500 iterations. A comparison among the real PSF, the initial PSF, and the final estimated PSF is presented in Fig. 3(d). It can be seen that the final estimated PSF is much better than the initial estimation and is similar to the true PSF. This similarity leads to the significant improvement of the restored image relative to the degraded image.

In Fig. 5 the image was blurred by a PSF of high-frequency vibrations in which the exposure duration

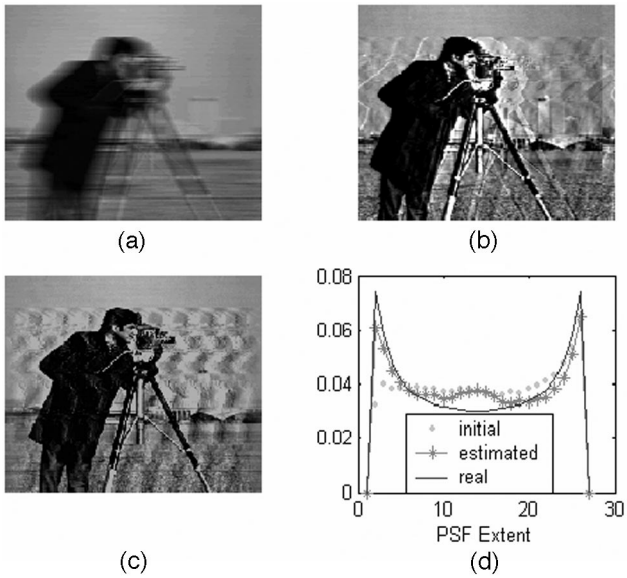


Fig. 5. Same as Fig. 3, but for a 27-pixel high-frequency sinusoidal motion blur type.

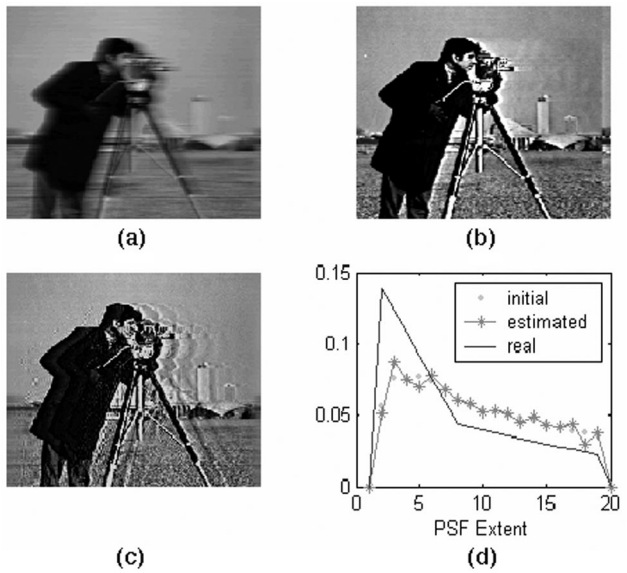


Fig. 6. Same as Fig. 3, but for another motion type obtained by using a different portion of a low-frequency sinusoidal blur with a 20-pixel extent and with a restoration using the EM iterative method.

is an integer multiple of the sinusoidal period or much higher. Again, the high similarity between the estimated PSF (with the RL method) and the true one [Fig. 5(d)] is indicated by the quality of the restored image [Fig. 5(c)]. In the last simulation example [Fig. (6)], the image was blurred by a portion of a sinusoidal vibration that behaves as an accelerated motion. The iterative deconvolution method here was the EM method, with 100 iterations. The last example (Fig. 7) shows a case of a real-motion-degraded image. The blurred image shown in Fig. 7(a) was taken from a moving car.[6] Figure 7(b) presents a comparison of PSFs estimated by the direct-only method and by the direct–iterative EM and the RL methods, assuming a 26-pixel blur extent pre-estimated by the direct method. In this case only small differences exist between the estimated PSFs. The restored images obtained from the direct–iterative EM and the direct–iterative RL methods are presented in Figs. 7(c) and 7(d), respectively.

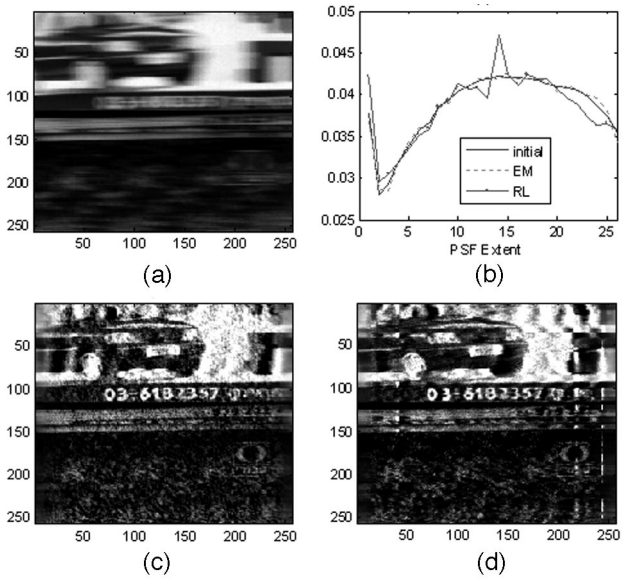


Fig. 7. (a) Real-motion-blurred image taken from a moving car,[6] (b) comparison of PSFs estimated by the direct-only method and by the proposed direct–iterative EM and RL methods for a blur extent estimated as 26 pixels, (c) image restored by the direct–iterative EM method, and (d) image restored by the direct–iterative RL method.

## 6. Conclusions

A main disadvantage of common iterative methods for image restoration (blind deconvolution) is their dependence on the required initial guess of the model parameters and in particularly the blur parameters. In this work, experimental examination of this drawback with the EM and the RL iterative methods was carried out (Section 3). It was found that the quality of the final estimated PSF clearly depends on the closeness of the initial PSF to the true PSF. Generally, an error in the initial PSF extent appears to have a more harmful effect than an error in its initial shape. Since the quality of the restored image (its closeness to the ideal image) is related directly to the quality of the final estimated PSF, any improvement of that estimated PSF leads to a better image restoration. From Section 3 we conclude that the iterative methods are likely to be improved when using a more accurate initial PSF than an arbitrary square pulse (a uniform-velocity motion PSF is usually used when no specific knowledge exists). From the examples of Section 5 we can see that the PSF estimation produced by the direct method will usually be improved (refined) by the iterative methods. Therefore the proposed combined direct–iterative process can usually improve the estimation of the original image, given only the degraded image. This improvement does not bear a higher computational load because, although the (added) complexity of the direct method is relatively low (when numerous iterations are performed), it will probably reduce the number of iterations.

## References

1. Y. Yitzhaky, R. Milberg, S. Yohayev, and N. S. Kopeika, "Comparison of direct blind deconvolution methods for motion-blurred images," Appl. Opt. **38,** 4325–4332 (1999).
2. D. Slepian, "Restoration of photographs blurred by image motion," Bell Syst. Tech. J. **46,** 2353–2362 (1967).
3. M. M. Sondhi, "Image restoration: the removal of spatially invariant degradations," Proc. IEEE **60,** 842–853 (1972).
4. M. Cannon, "Blind deconvolution of spatially invariant image blurs with phase," IEEE Trans. Acoust. Speech Signal Process. **ASSP-24,** 58–63 (1976).
5. Y. Yitzhaky and N. S. Kopeika, "Identification of blur parameters from motion blurred images," Graph. Models Image Process. **59,** 310–320 (1997).
6. Y. Yitzhaky, I. Mor, A. Lantzman, and N. S. Kopeika, "Direct method for restoration of motion-blurred images," J. Opt. Soc. Am. A **15,** 1512–1519 (1998).
7. M. I. Sezan and A. M. Tekalp, "Survey of recent develop-

ments in digital image restoration," Opt. Eng. **29,** 393–404 (1990).
8. G. Pavlovic and A. M. Tekalp, "Maximum likelihood parametric blur identification based on a continuous spatial domain model," IEEE Trans. Image Process. **1,** 496–504 (1992).
9. R. L. Lagendijk, J. Biemond, and D. E. Boekee, "Identification and restoration of noisy blurred images using the expectation-maximization algorithm," IEEE Trans. Acoust. Speech Signal Process. **38,** 1180–1191 (1990).
10. R. L. Lagendijk, A. M. Tekalp, and J. Biemond, "Maximum likelihood image and blur identification: a unifying approach," Opt. Eng. **29,** 422–435 (1990).
11. L. B. Lucy, "An iterative technique for the rectification of observed distributions," Astron. J. **79,** 745–754 (1974).
12. W. H. Richardson, "Bayesian-based iterative method of image restoration," J. Opt. Soc. Am. **62,** 55–59 (1972).
13. D. S. C. Biggs and M. Andrews, "Acceleration of iterative image restoration algorithms," Appl. Opt. **36,** 1766–1775 (1997).
14. A. P. Dempster, N. M. Laird, and D. B. Rubin, "Maximum likelihood from incomplete data," J. R. Stat. Soc. Ser. B Methodol. **39,** 1–38 (1997).
15. N. S. Kopeika, *A System Engineering Approach to Imaging* (SPIE Press, 1998).
16. W. K. Pratt, "Vector space formulation of two-dimensional signal processing operations," Comput. Graph. Image Process. **4,** 1–24 (1975).
17. N. B. Nill and B. H. Bouzas, "Objective image quality measure derived from digital image power spectra," Opt. Eng. **31,** 813–825 (1992).
18. P. Marziliano, F. Dufaux, S. Winkler, and T. Ebrahimi, "A no-reference perceptual blur metric," In *Proceedings of IEEE International Conference on Image Processing* (IEEE Press, 2002), Vol. 3, pp. 57–60.
19. Y. Yitzhaky and A. Stern "Restoration of interlaced images degraded by variable velocity motion," Opt. Eng. **42,** 3557–3565 (2003).
20. Y. Yitzhaky, G. Boshusha, Y. Levy, and N. S. Kopeika, "Restoration of an image degraded by vibrations using only a single frame," Opt. Eng. **39,** 2083–2091 (2000).